Hindawi Publishing Corporation
International Journal of Polymer Science
Volume 2016, Article ID 2610541, 15 pages
http://dx.doi.org/10.1155/2016/2610541

Research Article

Sulfonated Magnetic Nanocomposite Based on Reactive PGMA-MAn Copolymer@Fe_3O_4 Nanoparticles: Effective Removal of Cu(II) Ions from Aqueous Solutions

Reza Hasanzadeh,[1] Peyman Najafi Moghadam,[1] Naeimeh Bahri-Laleh,[2] and Ehsan Nazarzadeh Zare[3]

[1]*Department of Organic Chemistry, Faculty of Chemistry, Urmia University, Urmia, Iran*
[2]*Department of Polymerization Engineering, Iran Polymer and Petrochemical Institute (IPPI), P.O. Box 14965/115, Tehran, Iran*
[3]*Department of Chemistry, Faculty of Science, Gonbad Kavous University, Gonbad, Iran*

Correspondence should be addressed to Reza Hasanzadeh; reza.hasanzade7@gmail.com

Received 4 June 2016; Revised 2 August 2016; Accepted 3 November 2016

Academic Editor: Bernabé L. Rivas

Chelating magnetic nanocomposites have been considered as suitable materials for removal of heavy metal ions for water treatment. In this work poly(glycidyl methacrylate-maleic anhydride) copolymer (PGMA-MAn) is modified with 4-aminobenzenesulfonic acid (ABSAc) and subsequently the product reacted with modified Fe_3O_4 nanoparticles and 1,2-ethanedithiol (EDT) in the presence of ultrasonic irradiation for preparation of tridimensional chelating magnetic nanocomposite. Synthesized magnetic nanocomposite was characterized by Fourier transform infrared spectroscopy (FT-IR), scanning electron microscopy (SEM), X-ray diffraction analysis (XRD), vibrating sample magnetometer (VSM), energy dispersive X-ray analysis (EDX), elemental mapping analysis (EMA), Brunauer-Emmett-Teller (BET), and thermal gravimetric analysis (TGA). The adsorption behavior of Cu(II) ions was investigated by synthesized nanocomposite in various parameters such as pH, contact time, metal ion concentration, and adsorbent dosage. The equilibrium distribution coefficient (k_d) was determined and the findings prove that the k_d value is approximately high in the case of all selected metal ions. The synthesized nanocomposite exhibited good tendency for removing Cu(II) ions from aqueous solutions even at an acidic pH.

1. Introduction

All over the world, the adsorption of toxic metal ions pollutants from aqueous media is one of the major environmental and economic problems [1]. Heavy metals pollutants have developed a serious universal problem that endangers the environment and the health of human beings, due to their toxicity, carcinogenic effects, and tendency to bioaccumulate in living tissues particularly in human bodies. They can cause significant physiological disorders such as damage to central nervous system, production of energy, and irreversible damage of vital organs of body [2, 3]. About heavy metal pollution it should be also realized that, to prevent heavy metal poisoning, immediate detoxification of heavy metal wastewater through appropriate treatment is essential. Heavy metals are not decomposed by microbiological activities where they can be enriched by organisms and the type of bonding can be converted to more poisonous complexes (metal-organic) and the polluted areas can become spread by diffusion in the environment. Therefore, the removal of toxic metal ions from waters and wastewaters is essential in terms of safety of public health and environment [4].

Among heavy metal ions, copper is an essential trace element for human beings, yet it would become a great threat to public health with excessive ingestion. According to U.S. Environmental Protection Agency (EPA) and World Health Organization (WHO), the permissible limit of copper in drinking water is 1.3 and 2.0 mg dm^3, respectively [5]. Compared to pure copper, Cu(II) salts are more toxic because of

their water-soluble nature, with the main risks of gastrointestinal irritation, liver and kidney damage, and intravascular hemolysis. Their target organs are the gastrointestinal tract, cardiovascular and circulatory system, hematopoietic system, liver, kidneys, and nervous system [6].

Different methods of treating effluent containing Cu(II) have been developed over years which include coagulation, ion exchange, membrane separation, reverse osmosis, solvent extraction, chemical precipitation, and electroflotation [7]. However, most of these processes are unacceptable because of following reasons: disposal of sludge, their high cost, low efficiency, and inapplicability to a wide range of pollutants [8]. There are many types of adsorbents including natural materials (clays, zeolites, and lignite), activated carbon, silica gel, resins, polymeric hybrid sorbents, oxide minerals, fibers, biosorbents, and waste materials which have been used for adsorption of metal ions from aqueous solutions [9]. However, most adsorbents are nonselective and remove not only the target pollutants but also the minerals present in water. Thus, the topic necessitates the development of new polymeric adsorbents which have shown high performance and significant enhancement in toxic metal ion removal efficiencies from water [10].

Nowadays, among these methods, adsorption is the most promising technique due to its easiness, suitability, and high removal efficiency that make it a potentially cost-effective method for the elimination of toxic heavy metals from wastewater [11, 12]. Despite this, the development of novel adsorbents as nanomaterial with high performance is in great demand [13–15]. In the case of good performance of the removal of heavy metal ions with suitable functional groups magnetic nanomaterials combining magnetic separation and nanotechnology would be useful. Moreover, these magnetic nanomaterials as an adsorbent show excellent reusability after magnetic separation and the use of magnetic nanoparticles in treatment of wastewater is promising, due to high efficiency and cost effectiveness [16, 17].

Magnetic polymeric adsorbents are easy to be separated and have a relatively high surface area. They manipulate complex multiphase systems with an external magnetic field. A further step for developing adsorbents with superior properties would be the inclusion of magnetic particles into polymers, thus obtaining the advantages of both materials [24]. Recent studies indicated that nanomagnetic chelating polymers might be potential candidates as novel adsorbents. Functional polymers can be coated on the magnetic core to improve the stability of nanodispersions by preventing their aggregation; moreover, the absorption properties can be tailored by suitable functional groups [25, 26]. Therefore, an effective and simple method is urgently needed to synthesize modified magnetic polymeric nanomaterials with high saturation magnetization and relative large specific area which have good functional groups as binding sites (contain donors O, N, and S heteroatoms) for removal of heavy metals [27–30]. For this reason, a new reactive copolymer based on glycidyl methacrylate (GMA) and maleic anhydride (MAn) with reactive functional groups was applied for easy functionalization and also $-SO_3H$ group was selected as functional group for its effective adsorption of toxic metal ions by using sulfanilic acid compound [31, 32].

The objective of current research is to synthesize a chelating magnetic nanocomposite (CMN). A reactive PGMA-MAn copolymer was prepared by free radical copolymerization and the copolymer grafted by ABSAc. The grafted copolymer reacted with modified Fe_3O_4 nanoparticles and 1,2-ethanedithiol as modifier and cross-linker, respectively. The synthesized CMN was characterized and its ability to remove the Cu(II) ions from aqueous solutions was investigated at different conditions.

2. Experimental

2.1. Materials. Analytical grade glycidyl methacrylate (GMA), benzoyl peroxide (BPO), and maleic anhydride (MAn) were purchased from Sigma Aldrich Company. The GMA was distilled under reduced pressure before use. 3-Aminopropyl triethoxysilane (APTES) 99%, reagent-grade tetrahydrofuran (THF), n-hexane, ethanol, n-hexane, HCl, ammonia, and copper nitrate were purchased from Merck Company.

2.2. Equipment. IR spectra were measured with a Fourier transform infrared (FT-IR) spectrophotometer (Nexus – 670, Thermo Nicolet USA). The elemental analysis was performed by CHN analyzer (2400 series II, Perkin Elmer Company, USA). Surface area measurement was carried out by the Brunauer-Emmett-Teller method (BET) with Quantachrome TPRWin v1.0 (USA). The morphology of the nanocomposite was examined via scanning electron microscopy (SEM), (XL30 Philips Company, Netherland). The surface components of the samples were analyzed by using energy dispersive spectrometer (EDX) and element mapping analysis (EMA) (XL30 Philips Company, Netherland). The magnetic properties were measured with a vibrating sample magnetometer (VSM) (Lakeshore Cryotronics, Westerville, OH, USA) at room temperature in magnetic fields of up to 20 kOe. The X-ray diffraction (XRD) spectra were recorded on an X'pert Philips X-ray photoelectron spectrometer using nonmonochromated Mg Ka radiation as the excitation source (Netherland). Atomic absorption spectrophotometer (AAS), Shimadzu AA-6800 (Japan), was used for the determination of the metal ion concentrations in aqueous solutions. TGA analyses of prepared polymers were determined using the NETZSCH (Germany)-200 F3 Maia by scanning to 600°C with the heating rate of 10°C/min.

2.3. Preparation of 4-Aminobenzenesulfonic Acid (ABSAc). The ABSAc was prepared according to our previous work [32]. The brief description of synthetic method is as follows: typically, 10 g aniline in a 500 mL three-neck flask was fitted with a reflux condenser and a thermometer. Then 17.4 mL concentrated sulfuric acid was added to the flask slowly and cautiously. Afterwards the mixture was heated to about 170°C for 2.5 h. After the mixture was cooled to 50°C, it was poured into a beaker containing 100 mL of ice water. The ABSAc was purified by crystallization from hot water and then filtered and dried in vacuum oven at 60°C for 24 h.

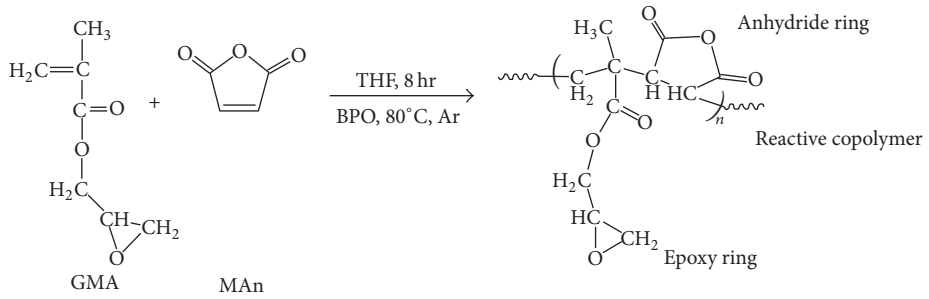

Scheme 1: The reaction of GMA and MAn for synthesis of the reactive PGMA-MAn copolymer.

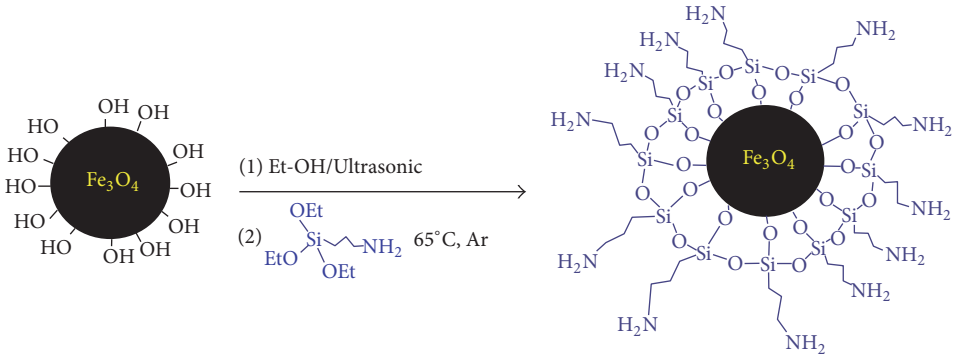

Scheme 2: Modification reaction of Fe_3O_4 magnetic nanoparticles by silanization reaction.

2.4. Synthesis of Glycidyl Methacrylate and Maleic Anhydride Copolymer (PGMA-MAn). Free radical copolymerization was used for the preparation of PGMA-MAn copolymer of GMA and MA in THF solvent according to our previous study [33]. The GMA and MA in molar ratio of 1 : 1 and THF (100 mL) were poured into a round-bottom flask equipped with a magnetic stirrer under an inert atmosphere. The reaction solution was degased through bubbling system with Ar for 30 min and then flask was placed in a preheated oil bath. The copolymerization processes were conducted at 80°C in the presence of BPO as initiator (1 mole %) for 8 hr. When the reaction was completed the solution was cooled (room temperature) and then the copolymer was precipitated in n-hexane as nonsolvent. Precipitated copolymer was separated from solvent by filtration. The filtrate (white-cream powder) was washed several times with n-hexane and dried in a vacuum oven at 40°C. Finally it was dried in a vacuum oven at 40°C until constant weight was achieved. The elemental analysis of final copolymer in molar ratio of 1 : 1 was measured and showed 54.78% C, 6.52% H, and 38.7% O. Scheme 1 shows the schematic of the fabrication route to prepare the copolymer.

2.5. Preparation of Fe_3O_4 Magnetic Nanoparticles. Fe_3O_4 nanoparticles were prepared by coprecipitation method [28] using $FeCl_2{\cdot}4H_2O$ and $FeCl_3{\cdot}6H_2O$ in 1 : 2 molar ratio. Ammonium hydroxide (30 mL) was mixed with deionized water (20 mL) which was deoxygenated by bubbling Ar for 20 min. In another beaker, 5.41 g $FeCl_3$ and 2.99 g $FeCl_2$ were dissolved in 50 mL deionized water. Then, the resultant solution was added drop-wise into the above-mentioned alkaline solution under vigorous stirring at 60°C. Ferrous and ferric chloride were allowed to react in ammonium hydroxide solution by alkaline coprecipitation and black precipitate was obtained. The formed black precipitate (Fe_3O_4) was harvested by magnetic bar, then washed three times with deionized water, and finally dried in vacuum oven at 50°C for 24 h.

FT-IR (KBr, ν cm^{-1}): 3365 (–OH), 674 (Fe–O).

2.6. Preparation of Amino Functionalized Fe_3O_4 Magnetic Nanoparticles (MNPs-NH_2) by Silanization Reaction. The prepared Fe_3O_4 magnetic nanoparticles (MNPs) were functionalized with 3-aminopropyl triethoxysilane for production of nanoparticles that contain amine groups [34]. These functional groups increase the availability of amine functions for the complexation of metal ions as well as sulfate groups in polymer structure. A long time is needed for the reaction between a liquid alkoxysilane and solid nanoparticles as a heterogenic reaction (silanization). In this case, the nanoparticles (1.50 g) were dispersed in ethanol (150 mL) ultrasonically in a water bath under Ar atmosphere for 45 min. The resultant dispersion was bubbled with argon gas for 30 min and then 3-aminopropyl-triethoxysilane (13 mmol, 3 mL) compound was added into the mixture and the mixture was sonicated for 1 hr and then heated at 50°C under magnetic stirring for 24 hr. Modification reaction of MNPs was shown in Scheme 2. Lastly, modified MNPs were washed by acetone and deionized water for several times and dried in vacuum oven at 60°C for 24 h. Scheme 2 shows modification reaction of MNPs.

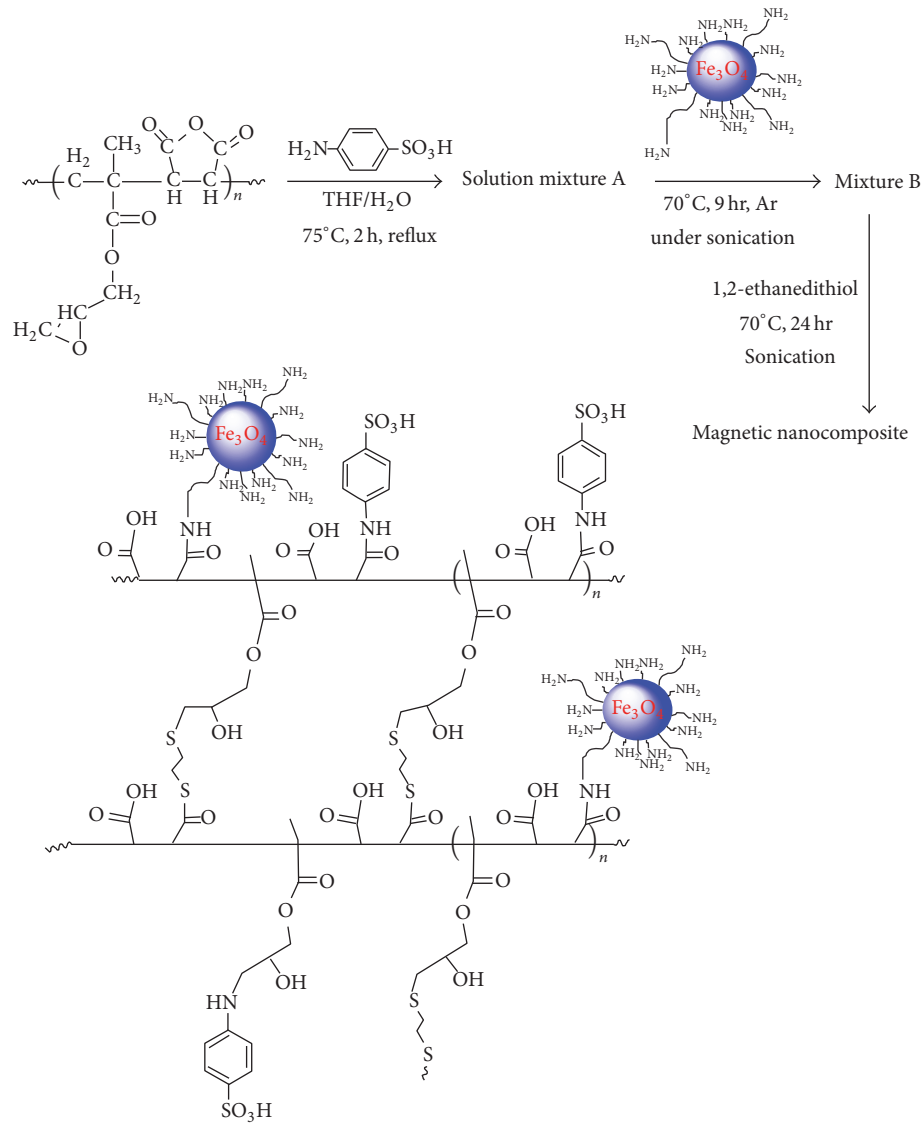

Scheme 3: Reaction mechanism for synthesis of PGMA-MAn/ABSAc@Fe_3O_4 nanocomposite.

2.7. Synthesis of PGMA-MAn/ABSAc@Fe_3O_4 Magnetic Nanocomposite Adsorbent. PGMA-MAn/ABSAc@Fe_3O_4 magnetic nanocomposite was synthesized by reaction of PGMA-MAn copolymer (2 g) and ABSAc (1 g) in THF/H_2O solvent at 80°C (solution A). In separate flask MNPs-NH_2 (0.15 g) were sonicated for 45 min in 10 mL of water to obtain dispersed MNPs (solution B). Then solution A was added to solution B under ultrasonic irradiation and the mixture was kept at 80°C for 12 h under stirrer. Subsequently 1,2-ethandithio (1 mL) as cross-linker was added drop-wise to the mixture and the reaction was carried out at reflux condition for 24 hr. Finally the resulting PGMA-MAn/ABSAc@Fe_3O_4 nanocomposite was separated by external magnetic field, washed with deionized water and acetone several times, and dried in vacuum oven at 50°C for 48 h. The synthesis reactions are shown in Scheme 3.

2.8. Adsorption Measurement. For the synthesized PGMA-MAn/ABSAc@Fe_3O_4 nanocomposite, the adsorption experiments was measured via a batch method for Cu(II) ions. The effect of different pH range [2–7], contact time (5–60 min), adsorbent dosage (3–20 mg), and initial concentration 1–25 mg/L on the removal of Cu(II) ions was investigated by the prepared nanocomposite. The solutions were prepared using dilutions of the stock solution. The effect of each factor was shown under constant conditions of 10 mg of adsorbent powder dispersed in 25 mL of Cu(II) solution (50 mg L^{-1}) for 20 min with stirring at 150 rpm and 298 K, varying the initial level of related factor. After equilibrium was reached in all the experiments, the two phases were separated and the concentration of Cu(II) analyzed using AAS. The equilibrium time was less than 20 min. Scheme 4 shows the proposed

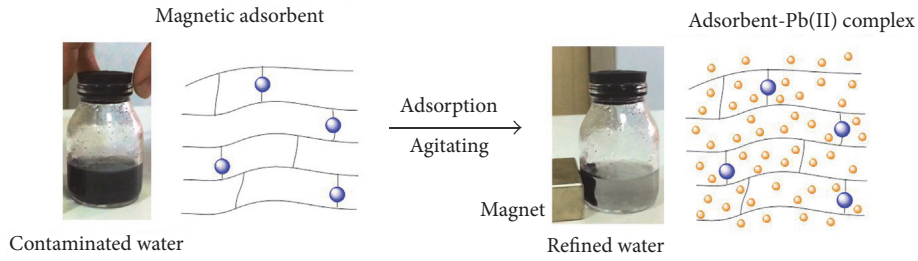

Scheme 4: The proposed adsorption efficiency of the PGMA-MAn/ABSAc@Fe_3O_4 nanocomposite in removal of Cu(II) ions.

adsorption mechanism of Cu(II) from water by PGMA-MAn/ABSAc@Fe_3O_4 nanocomposite. Each measurement was repeated three times and the reported results were their average values. The adsorption percentage of Cu(II) was calculated using the following equation:

$$\%\ \text{heavy metal ions removal} = \left(\frac{C_0 - C_e}{C_e}\right) \times 100, \quad (1)$$

where C_0 and C_e are the initial and equilibrium concentration (mg/L) of the Cu(II) metal ion solution, respectively.

3. Results and Discussion

3.1. Characterization of the Prepared Materials

3.1.1. SEM. Figures 1(a), 1(b), and 1(c) show the SEM image of the bare Fe_3O_4, copolymer, and PGMA-MAn/ABSAc@Fe_3O_4 nanocomposite. It can be seen, from Figure 1(a), that Fe_3O_4 particles have a nearly spherical shape with a size distribution of around 60–150 nm in diameter. It can be seen that Fe_3O_4 particles have a nearly spherical shape. Magnetic bare Fe_3O_4 particles have hydrophobic surfaces with a large surface area to volume ratio, so this leads to agglomeration of particles and formation of large clusters, resulting in increased particle size. Representative images of the PGMA-MAn copolymer in Figure 1(b) reveal bulk morphology with small clusters of irregular clots in microscale. So, it can be acclaimed that in consequence of GMA and MAn copolymerization an amorphous white-cream cluster with a porous structure was formed and the copolymer apparently exhibited the uniform morphology with connected particles.

It was observed that surface morphology of prepared magnetic nanocomposite differed from the unmodified Fe_3O_4 nanoparticles and copolymer (Figure 1(c)). The surface irregularity of the synthesized nanocomposite and the formed sheet structure of it can be due to cross-linking process and presence of nanoparticles and 1,2-ethanedithiol into the composite structure. It seems that the MNPs-NH_2 nanoparticles in composite structure were multidispersed in sheets with thickness of about 50 nm.

The SEM image of nanocomposite-Cu(II) complex after adsorption is shown in Figure 1(d). This image showed curly and irregular sheets on the surface of the PGMA-MAn/ABSAc@Fe_3O_4 nanocomposite. After the adsorption of Cu(II) metal ions, surface of the nanocomposite was evenly packed with this metal ion and the bead structure was slightly longer apparent which indicates that the active sites such as amine, sulfide, and sulfate groups existed on the protruding portions of the surface. The resulting a smooth surface on irregular sheets (with slight increasing the thickness size) indicates the suitable interactions of Cu(II) ions with the active sites of prepared nanocomposite.

3.1.2. XRD. The XRD patterns of the prepared Fe_3O_4 nanoparticles, the copolymer, and PGMA-MAn/ABSAc@Fe_3O_4 were used for phase confirmation (Figure 2). The reflection peak positions and relative intensities of the magnetic nanoparticles (MNPs) agree well with XRD patterns for Fe_3O_4 MNPs in the literature [35]. In addition, the XRD patterns of the Fe_3O_4 MNPs and PGMA-MAn/ABSAc@Fe_3O_4 nanocomposite have same peak positions, indicating that during nanocomposite preparation the phase of the Fe_3O_4 MNPs does not change.

3.1.3. BET. According to BET measurements, the specific surface areas of Fe_3O_4 nanoparticles, PGMA-MAn copolymer, and PGMA-MAn/ABSAc@Fe_3O_4 nanocomposite were 86.711, 8.233, and 21.265 m^2/g, respectively. Significant reduction in the surface area of the prepared PGMA-MAn/ABSAc@Fe_3O_4 nanocomposite confirms size enlargement of Fe_3O_4 particles during coating process by modified copolymer and final cross-linking.

3.1.4. FT-IR. Also, the preparation of the PGMA-MAn/ABSAc@Fe_3O_4 nanocomposite was confirmed by FT-IR technique. The FT-IR spectra of the ABSAc, bare Fe_3O_4, MNPs-NH_2, PGMA-MAn, and PGMA-MAn/ABSAc@Fe_3O_4 have been depicted in Figures 3(a)–3(e), respectively. In Figure 3(a) the absorption peaks of 780, 1000, 1150, 1230, 1260, 1470, and 1600 were attributed to the C–S, S–OH, SO_3H, O=S=O, C–N, and C=C groups, respectively, in ABSAc compound. As is clear from Figure 3(b), the peaks of 500–750 cm^{-1} belong to the Fe_3O_4 [28]. The appeared bands at 3210 to 3550 cm^{-1} and 1019 cm^{-1} can be attributed to the OH groups that covered the Fe_3O_4 nanoparticles. As can be seen from Figure 3(c), presence of two peaks at 3209 and 3330 cm^{-1} (stretching vibration of NH_2 group) confirms the synthesis of MNPs-NH_2 with terminal amine groups. The Fe–O–Si adsorption band which appeared around 584 cm^{-1} was covered with the Fe–O vibration of Fe_3O_4 nanoparticles.

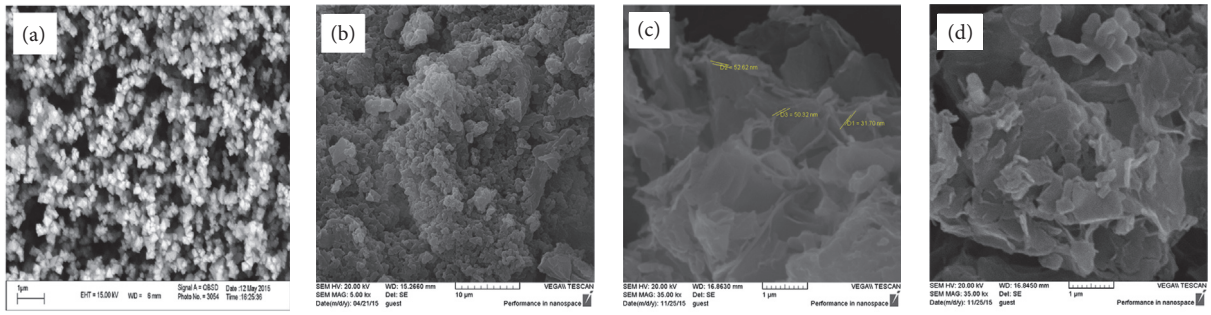

(a) (b) (c) (d)

Figure 1: The SEM micrographs of Fe_3O_4 nanoparticles (a), PGMA-MAn copolymer (b), and PGMA-MAn/ABSAc@Fe_3O_4 nanocomposite before (c) and after (d) complexation with Cu(II) ions.

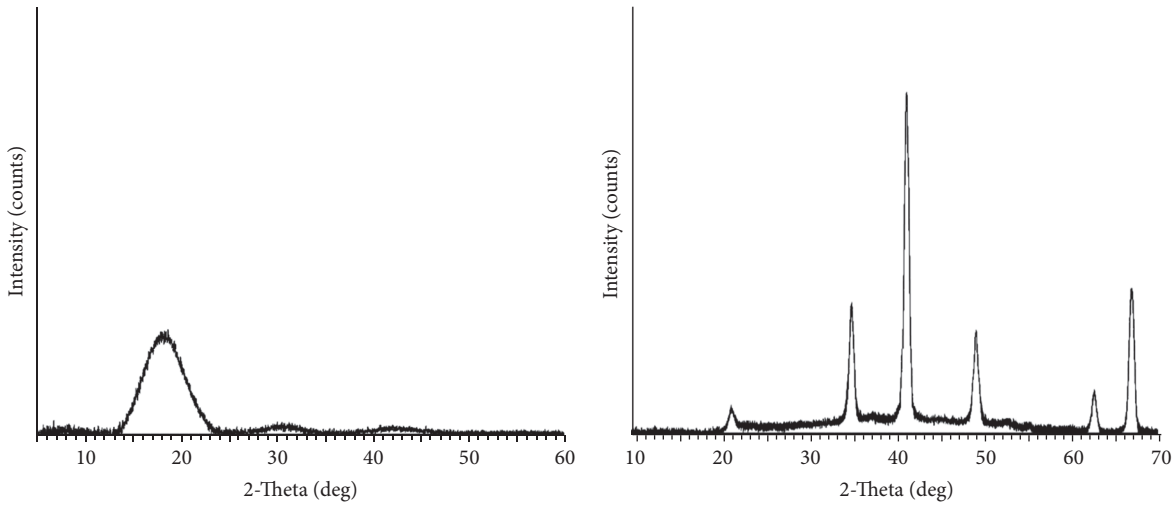

(a) (b)

Figure 2: XRD patterns of the PGMA-MAn copolymer and PGMA-MAn/ABSAc@Fe_3O_4 nanocomposite.

The significant difference for this spectrum with bare Fe_3O_4 was the appearance of the bands at 1085, 810, and 480 cm^{-1} which was attributed to the bending vibration, symmetric stretching vibration, and asymmetric stretching vibration of Si–O–Si groups, respectively. Absorption peak of aliphatic CH_2 appeared at 2923 cm^{-1}. The similarity between Figures 3(b) and 3(c) spectra clearly confirms that APTES has been successfully bonded to the surface of Fe_3O_4 nanoparticles.

In the case of copolymer spectrum the peaks observed at the range of 2999–2874 cm^{-1} are attributed to the asymmetrical and symmetrical C–H stretching of aliphatic methine, methylene, and methyl groups (Figure 3(d)). The C=O stretching of the ester groups (related to GMA portion) is observed at 1730 cm^{-1}. Anhydride C=O peaks appeared as band intensity at 1855 and 1783 cm^{-1}. The peaks at 1256 and 1150 cm^{-1} are due to –C–O stretching. The C–O–C stretching of the epoxide appeared at 910–848 cm^{-1}. The asymmetrical and symmetrical bending vibrations of methyl group are seen at 1460–1340 cm^{-1}, respectively.

In Figure 3(e), the peaks at about 3430–3455 are attributed to OH and NH stretching vibration. The peaks at 3198, 1730, 1705, and 1650 cm^{-1} are ascribed to amide group (stretching vibration of N–H), C=O bond of ester, carboxylic acid, and amid group, respectively. In addition, disappearance of anhydride peaks clearly shows the synthesis of nanocomposite. In Figure 3(e), appearance of ester peak (1730), O=S=O peak (1280), $–SO_3H$ (1240–1170), S–OH (990), C–S (820), and Fe–O (590 cm^{-1}) peak demonstrates that the nanocomposite was successfully synthesized. The stretching of S=O group can appear at 1035 and 505 cm^{-1} which have overlapped with other peaks. Also appearance of amid peak indicated that amine group of ABSAc was opened the anhydride groups.

3.1.5. EDX. The components of the synthesized PGMA-MAn/ABSAc@Fe_3O_4 were analyzed by the EDX too, and the results are shown in Figure 4(b). The characteristic peaks of C, N, O, Si, Fe, and S show that the magnetite nanoparticles have been coated by polymer matrix. This analysis could be

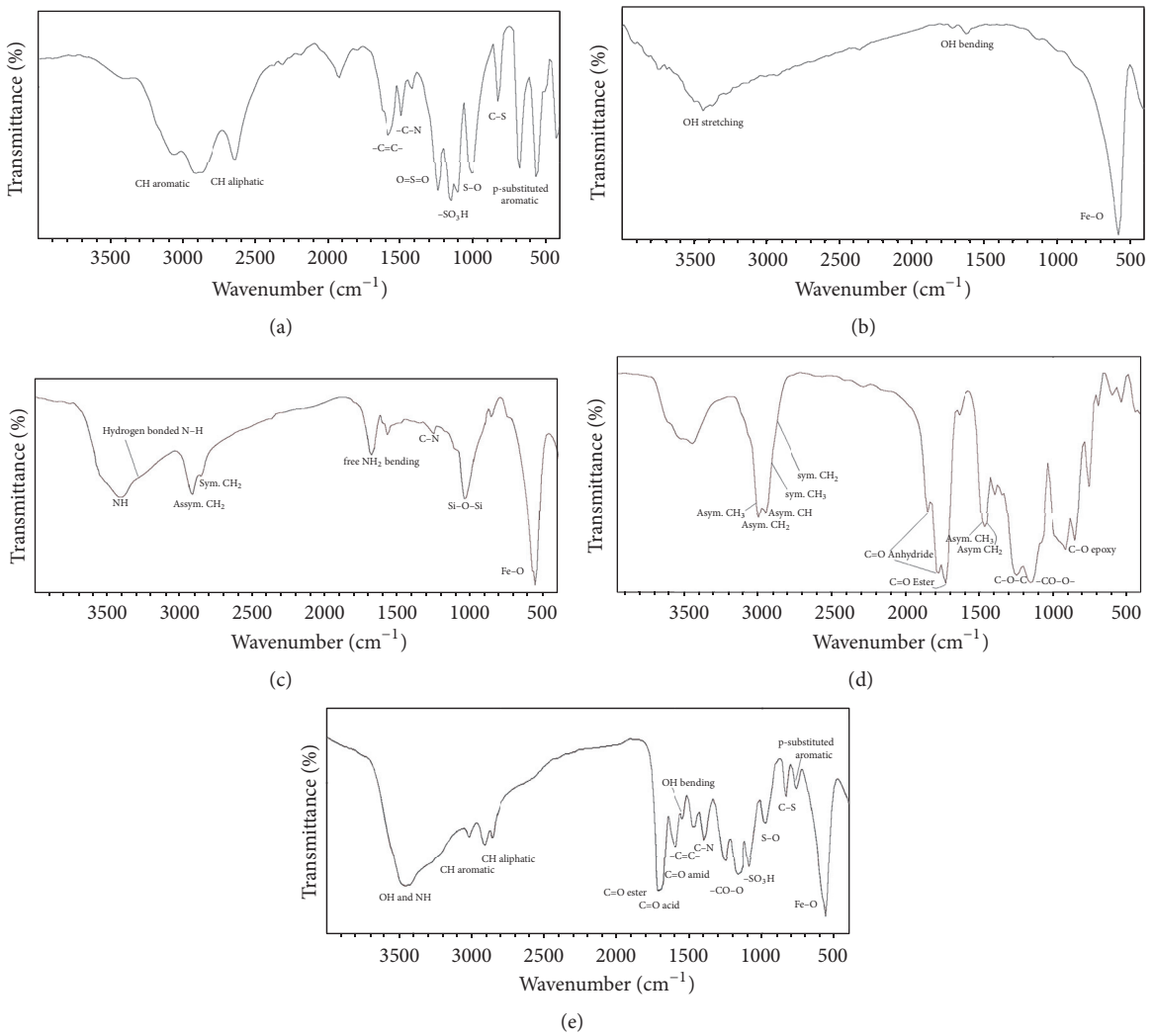

Figure 3: FT-IR spectra of ABSAc, bare Fe_3O_4, MNPs-NH_2, PGMA-MAn, and PGMA-MAn/ABSAc@Fe_3O_4 nanocomposite.

another evidence for successful preparation of the nanocomposite.

Element mapping analysis (SEM-EDX) was used for determination of element distribution on the surface of nanocomposite beads. This analysis was carried out on a cross-sectioned nanocomposite bead and the results are shown in Figure 4(c). These images indicate the presence of some elements which confirm the synthesis of PGMA-MAn/ABSAc@Fe_3O_4 nanocomposite.

3.1.6. VSM. Isolation of magnetic nanoparticles sorbents from solutions is possible easily by using a magnet, so the magnetization power of sorbents is essential. Saturation magnetization (M_S) value of Fe_3O_4 nanoparticles was 63 emu/g. The surface of Fe_3O_4 nanoparticles was coated with aminopropyltriethoxysilane compound which leads to a decrease in saturation magnetization value of MNPs-NH_2. The saturation magnetization values of modified MNPs and nanocomposite were determined 59 and 31 emu/g, respectively, and compared with the original nanoparticles. Figure 5 shows the magnetization curve as a function of perpendicular magnetic field for bare Fe_3O_4, Fe_3O_4–NH_2, and PGMA-MAn/ABSAc@Fe_3O_4 nanocomposite at room temperature.

Both modified nanoparticles and nanocomposite curves show a smaller magnetic properties value as compared to uncoated Fe_3O_4 nanoparticles which provides evidence of the formation of a silane compound and polymer matrix around the Fe_3O_4 nanoparticles. Since the polymer matrix was diamagnetism, it was reasonable that the ratio of paramagnetic content decreased, which led to lower saturation moments than that of the bare Fe_3O_4. It is well known that small coercivity (Hc) and remanence (Mr) in the absence of the external magnetic field indicated the super-paramagnetic property of materials [27]. Therefore, according to the obtained results, it was concluded that both MNPs-NH_2 nanoparticles and PGMA-MAn/ABSAc@Fe_3O_4 nanocomposite were super-paramagnetic.

The synthesized nanocomposites (with many –COOH, $–SO_3H$, and $–NH_2$ groups) were uniformly dispersed in aqueous solution in the absence of magnetic field. To further

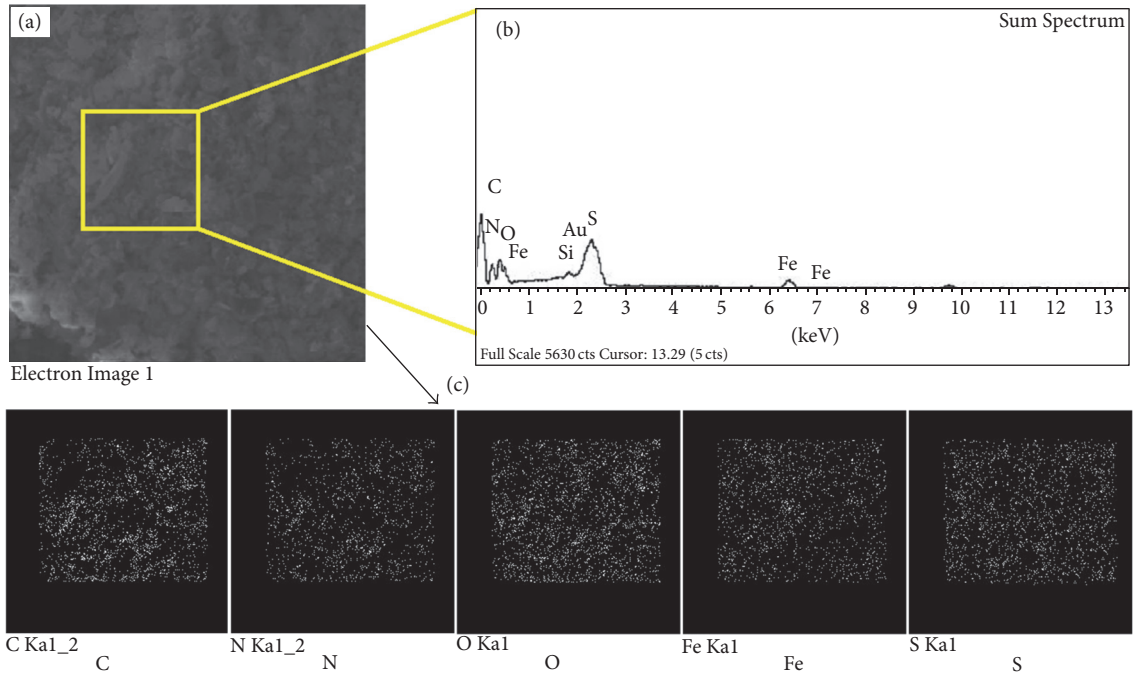

Figure 4: (a) Electron image for (b) EDX analysis and (c) element mapping analysis of PGMA-MAn/ABSAc@Fe_3O_4 nanocomposite.

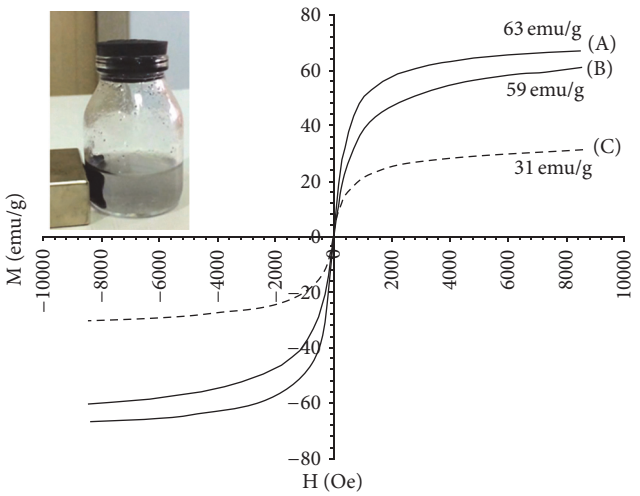

Figure 5: VSM of bare Fe_3O_4 nanoparticles, MNPs-NH_2, and PGMA-MAn/ABSAc@Fe_3O_4 nanocomposite.

investigate the performance of the magnetic nanocomposite under magnetic environment, the nanocomposite was dispersed in water that obtained dark black dispersion. Then a magnet was placed near the cuvette to separate the nanocomposites. The nanoparticles were completely aggregated to the cuvette wall within about 20 sec, and the dispersion became clear and transparent (Figure 6). The prepared nanocomposite with good magnetic properties and suitable functional groups suggests that it can probably be applied for any kind of magnetic field-guided targeting.

3.2. Thermogravimetric Analysis (TGA). Thermogravimetric analysis (TGA) was used to evaluate the thermal stability of synthesized materials. Figure 7 demonstrates the TGA thermograms of Fe_3O_4 nanoparticles, MNPs-NH_2, PGMA-MAn copolymer, and PGMA-MAn/ABSAc@Fe_3O_4 nanocomposite under nitrogen atmosphere (from 50°C to 800°C by heating rate of 10°C/min). As shown in Figure 7(a) the bare Fe_3O_4 nanoparticles show a weight loss of about 1.7% at temperatures of 50 to 200°C which can be related to the loss of physically adsorbed water. The weight loss, 1.4% at 700–800°C, may be attributed to the thermal crystal phase transformation from Fe_3O_4 to γ-Fe_2O_3. In the case of the MNPs-NH_2 it can be observed that three steps occurred (Figure 7(a)). The initial step at 50–210°C was related to the loss of water. The two latter weight losses (210–300°C and 300–800°C) were attributed to decomposition of the 3-Aminopropyl triethoxysilane portion anchored to the Fe_3O_4 which confirmed the reaction of silane compound with Fe_3O_4 nanoparticles.

Figure 7(b) indicates the TGA of PGMA-MAn copolymer. In this figure there is one thermal decomposition which can be related to entire decomposition of the copolymer (degradation of pendent ester groups (–COOR), loss of CO_2, and decomposition of the main chain of polymer).

In the TGA curve of the PGMA-MAn/ABSAc@Fe_3O_4 nanocomposite (Figure 7(c)), the weight loss of absorbed physical and chemical water (7%) was shown below 190°C. Then degradation of the nanocomposite network begins at about 220°C and final decomposition occurred around 450–610°C (the weight loss is significant by about 73%). There is no significant weight loss from 610 to 800°C, implying the presence of only Fe_3O_4. The TGA was also used to determine

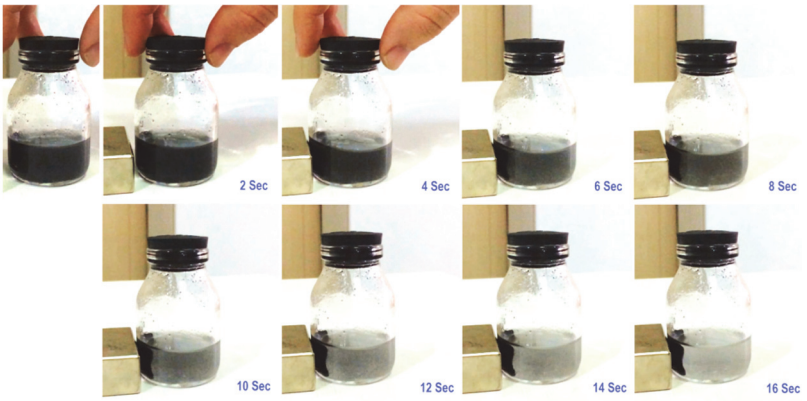

Figure 6: Rapid separation of magnetic nanocomposite from solution phase.

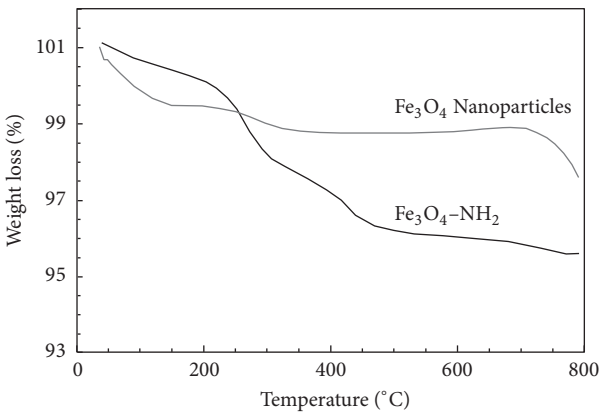

(a)

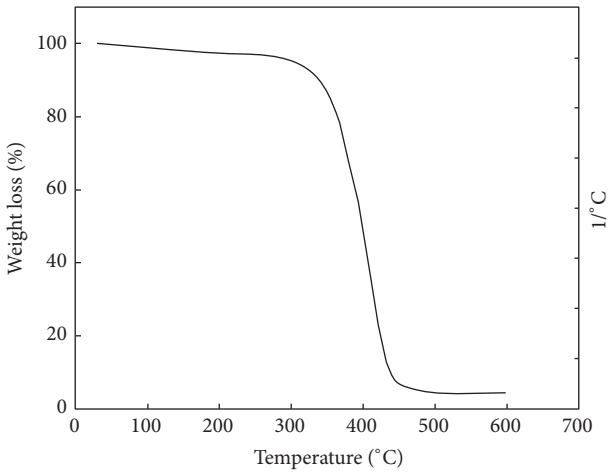

(b)

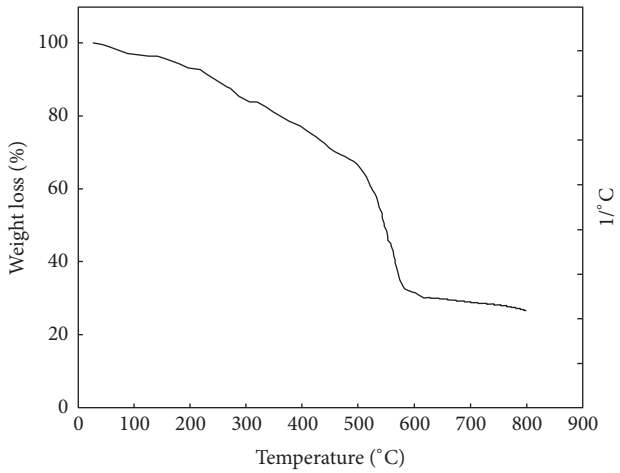

(c)

Figure 7: TGA thermograms of (a) bare Fe_3O_4 nanoparticles and MNPs-NH_2, (b) PGMA-MAn copolymer, and (c) PGMA-MAn/ABSAc@Fe_3O_4 nanocomposite.

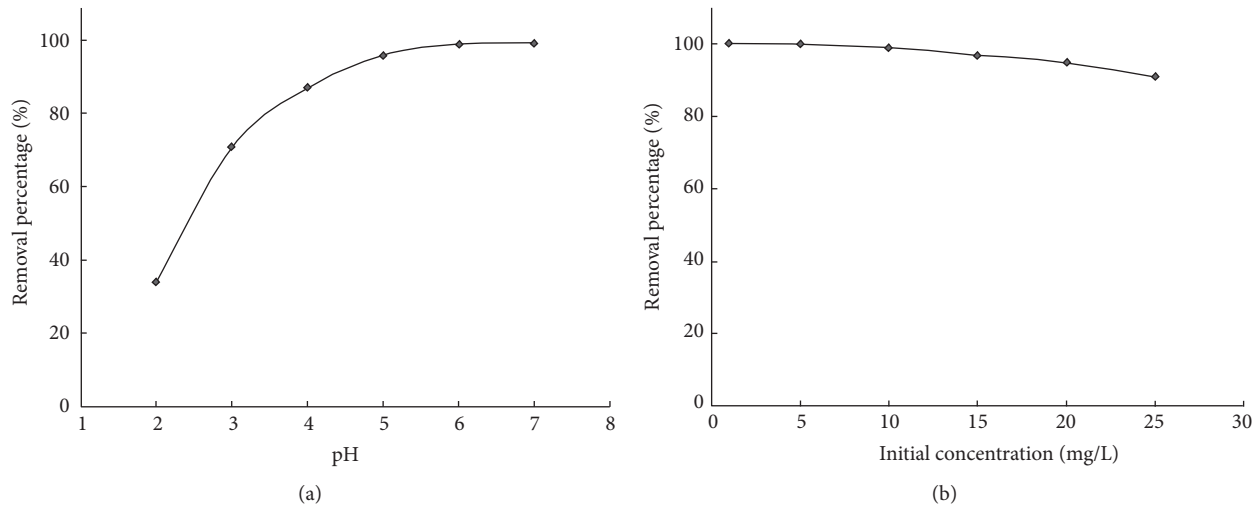

Figure 8: Effect of (a) pH and (b) initial concentration of Cu(II) on the removal percentage of Cu(II).

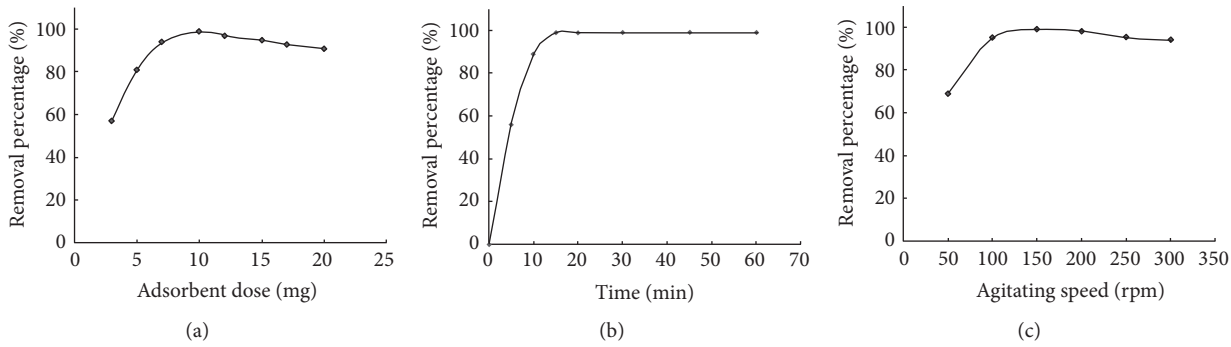

Figure 9: Effect of adsorbent dosage (a), shaking time (b), and agitating speed (c) on the removal percentage of Cu(II).

the weight percentage of Fe_3O_4 in the nanocomposite beads. The results indicated that the Fe_3O_4 content of nanocomposite beads can be up to 20 wt%.

3.3. Effect of Different Parameters in Adsorption of Cu(II) Ions by the Synthesized PGMA-MAn/ABSAc@Fe_3O_4 Nanocomposite

3.3.1. pH. Adjusting the pH of the metal ion solutions has significant effect on the removal efficiency of the PGMA-MAn/ABSAc@Fe_3O_4 as adsorbent for metal ion, because at low pH values (lower than 4) protonation of the oxygen and nitrogen atoms of the active sites decreases the binding ability of the active sites toward Cu(II) ions. On the other hand, at pH values higher than 7, Cu(II) may form hydroxide precipitates. Figure 8(a) demonstrates the influence of pH of test solution on the adsorption of Cu(II) by PGMA-MAn/ABSAc@Fe_3O_4 nanocomposite at pH 2–7. As it is clear from Figure 8, there are noteworthy increases in removal efficiency of the Cu(II) ions with increasing pH values of the test solution from 2 to about 6. At pH values higher than 6, the removal efficiency value of Cu(II) is approximately constant. To achieve optimum removal efficiency and prevent the risk of the hydroxide precipitation of the Cu(II) ions, in the subsequent experiments, pH value of 6 was selected as the optimum value for the removal of Cu(II). The pH of the solutions was adjusted by the use of acetic acid/sodium acetate buffer.

3.3.2. Metal Ion Concentration. The rate of adsorption is an imperative factor for effective adsorption and depends on the initial concentration of metal ion [12]. The removal percentage of Cu(II) by PGMA-MAn/ABSAc@Fe_3O_4 at different concentrations (1–25 mg/L), keeping all other factors constant, is revealed in Figure 8(b). By increasing the metal ion concentration the removal percentage of metal ion was increased up to 10 mg/L. Further increase in the concentration of metal ions was accompanied by reduction in the removal percentage and this phenomenon may be due to saturation of the functional groups in adsorption sites of the adsorbent with the Cu(II) ions at higher concentrations.

3.3.3. Agitation Speed. The effect of agitation speed was also investigated at room temperature. As shown in Figure 9(a) it was observed that by increasing the agitation speed from 50 to 300 rpm, the maximum removal percentage of Cu(II) ions was obtained up to 150 rpm. Hence, at a agitation speed

between 100 and 150 rpm, maximum adsorption was obtained, with 99% removal of Cu(II). This result can be due to the fact that increase in agitation speed enhanced diffusion of metal ions to the surface of the adsorbent and also caused reduction of the boundary layer film around the adsorbent.

3.3.4. Shaking Time. The importance of shaking time comes from the need to identify the possible rapidness of binding and removal processes of the investigated metal ions by the synthesized adsorbents and to obtain the optimum time for complete removal of the target metal ions. Effect of contact time on Cu(II) ions removal by PGMA-MAn/ABSAc@Fe_3O_4 was studied by variation of the contact time (1 to 60 min) for constant initial concentrations (10 mg/L). Figure 9(b) shows the removal percentages of Cu(II) ions as a function of contact time. The results showed that shaking time of 15 min was enough for complete removal of metal ions from 50 mL solution with concentration of 50 mg/L for Cu(II) ions. The rapid removal of adsorbate at the first 15 min of contact accounted for 99% was obtained for the total sorption (49.51 mg/g) at equilibrium as adsorption capacity (mg/g). Adsorption capacity of prepared magnetic nanocomposite was determined with (2) as follows:

$$q_e = (C_0 - C_e)\frac{V}{m}, \tag{2}$$

where C_0 and C_e are the initial and equilibrium concentration of metal ions (mg/L) at initial and equilibrium time, respectively; V and m are volume of the solution (L) and the weight of adsorbent (g), respectively. The abundant availability of active sites on the nanocomposite can be reason of the rapid phase, whereas adsorption becomes less efficient with the gradual occupancy of these active sites, during the slower phase. Adsorption of Cu(II) ions is found to be proportionate to the contact time up to equilibrium achieved, after which it is independent of time because of the fact that the rate of adsorption and desorption will be same at equilibrium. This relatively fast sorption of Cu(II) on the prepared nanocomposite probably reflects high accessibility of this metal ion to the ion exchange sites in PGMA-MAn/ABSAc@Fe_3O_4.

3.3.5. Adsorbent Dose. The amount of adsorbents is very important parameter as it determines the extent of metal ion adsorption and maybe used to define the cost of adsorbent per unit volume of solution to be treated [28]. The removal percentage for Cu(II) ion was investigated as a function of adsorbent dosage and the results are shown in Figure 9(c). From the experimental data it can be deduced that the adsorption of the Cu(II) increased with increasing the amount of adsorbents. This increase in the adsorption could be due to presence of more binding sites on the surface of adsorbents to form complexes with Cu(II). It may be deduced from these results that, at lower adsorbent dosage (below 10 mg), the metal ions were competing for sorption by functional groups at limiting sorption sites. By increasing the amount of adsorbent, the availability of sorption sites eased resulting in greater removal percentage of metal ions. However further increase in the mass of adsorbent did not result in sufficient enhancement in the sorption capacity of the prepared nanocomposite for these metal ions. However, the optimum amount of the nanocomposite for further adsorption experiments was selected as 10 mg, due to the maximum adsorption happening for 10 mg of adsorbents and further increase in adsorbent dosage had less influence on removal of Cu(II). This can probably suggest that adsorption of Cu(II) occurs mostly with active sites on the surface of samples.

3.4. Investigation of Nanocomposite-Cu(II) Complex by FT-IR and EDX Analyses. FT-IR and EDX techniques can be used for confirmation of the adsorption process by synthesized chelating nanocomposite. The FT-IR spectroscopy has been used for the characterization of nanocomposite metal complexes because of the frequency at which a characteristic group of the polymer absorbs is modified by metal ion complexation, the shift or absence of a certain band present in the starting ligand, and the presence of new bands being observed. Therefore, the first information about the structural changes caused by the complexation of obtained chelated resin with Cu(II) was provided by FT-IR spectra.

The shift of infrared absorption bands for the free carbonyl bond (C=O) of the carboxylate and amide groups can be observed in FT-IR spectrum. In Figure 10-I (a and b) it seems that, due to the chelation of Cu(II) ions with nanocomposite, the absorption peaks of various carbonyl groups (ester and groups) overlapped with each other, and they appeared as broad peak at about 1735–1650 cm^{-1}. After the chelating process, the FT-IR shows that, at the result of nitrogen ion pair incorporation (acid and amide) in this process, the carbonyl absorption of acid and amide absorption peak in FT-IR has blue shifted. The absorption bands at 1176, 1123, and 1011 cm^{-1} which are related to O=S=O, C–S, and S–OH, respectively, have no change after chelation. Also, the absorption bands characteristics for the aromatic parts of the matrix were not influenced by the metal complexation.

The EDX technique was used to explain the mechanisms of Cu(II) adsorption onto the chelating magnetic nanocomposite. In Figure 10-II(a), the new peaks of Cu(II) in spectrum demonstrated that this metal ion was loaded on the prepared nanocomposite. This result confirmed the presence of Cu(II) metal ions on the surface of adsorbent. Elemental mapping analysis demonstrates the presence of Cu(II) ions in adsorbent which can be seen in Figure 10-II(b). The proposed mechanism for interaction of PGMA-MAn/ABSAc@Fe_3O_4 nanocomposite with Cu(II) ions is shown in Scheme 5. There are electron donor atoms such as oxygen and nitrogen in the adsorption sites of the synthesized nanocomposite which can interact with metal ions. It can be said that the electron of HOMO orbital (donor atoms) can come to LUMO orbital of acceptor atoms (metal ions). At the result of this process complex nanocomposite metal can be formed.

3.5. Determination of the Equilibrium Distribution Coefficient, k_d. For investigation of metal cation mobility by adsorbent, k_d value can be used as a valuable tool. High values of distribution coefficient, k_d, indicate that the metal ions have been

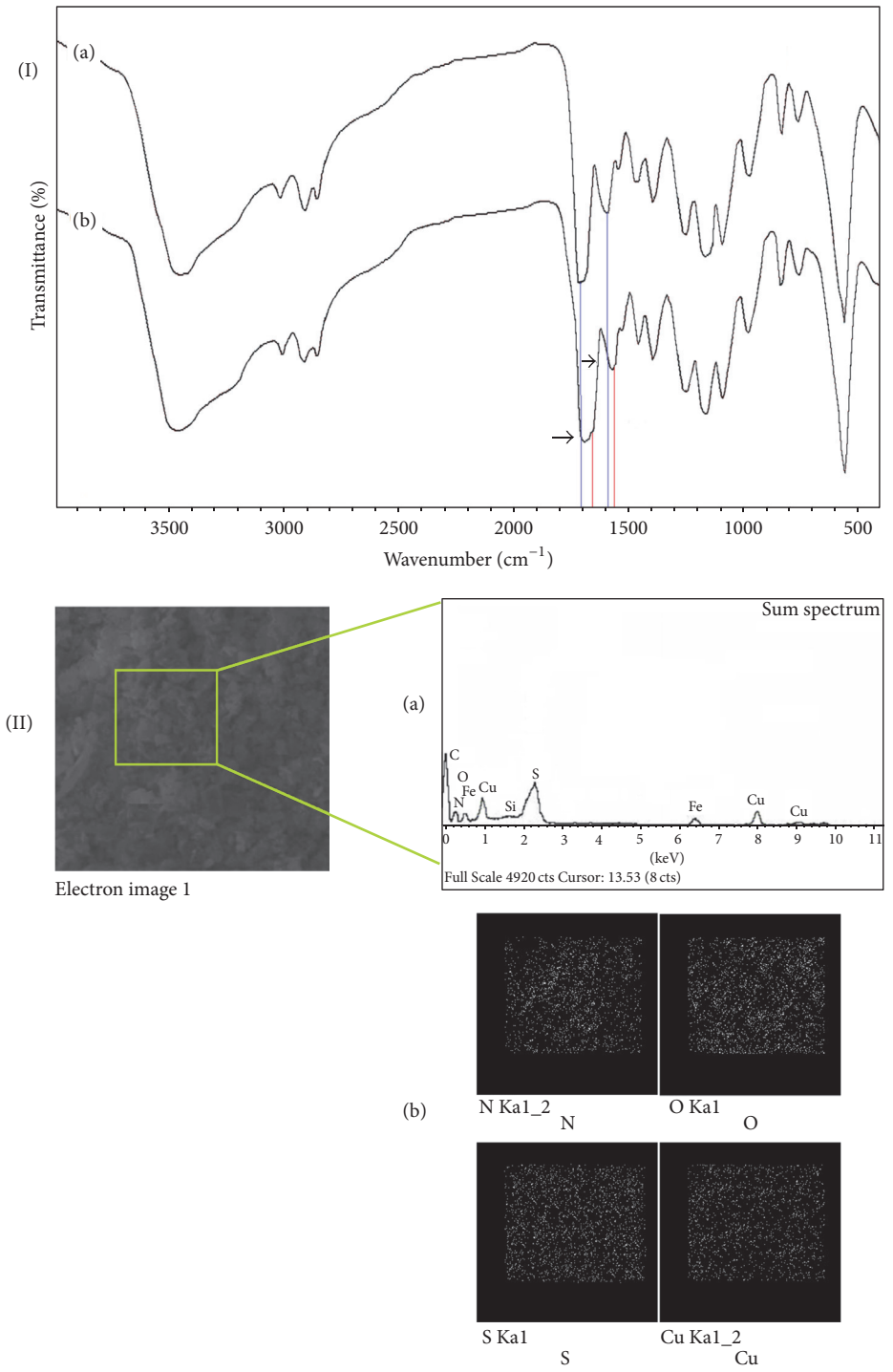

Figure 10: (I) FT-IR spectra of (a) prepared magnetic nanocomposite and (b) complex of nanocomposite-Cu. (II) (a) EDX analysis and (b) EMA image of the nanocomposite-Cu(II) complex.

retained by the adsorbent as solid phase, while low values of, k_d, indicate that a large fraction of the metal remains in the solution phase. The distribution coefficient k_d was calculated using the fallow equation [36]. k_d (in the unit of mL/g throughout) is simply a mass-weighted partition coefficient between the solid phase and the liquid supernatant phase as follows:

$$k_d = \frac{\text{amount of metal ion in the adsorbent}}{\text{amount of metal ion in the solution}} \times \frac{V}{m}, \quad (3)$$

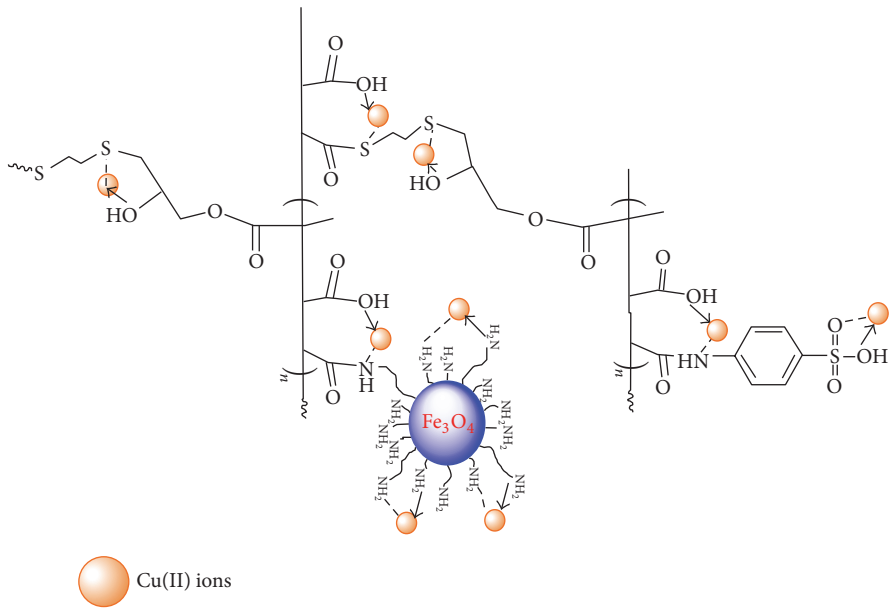

Scheme 5: The proposed mechanism for interaction of PGMA-MAn/ABSAc@Fe_3O_4 nanocomposite with Cu(II) ions.

Table 1: Distribution coefficient, k_d, of Cu(II) ions adsorption by magnetic nanocomposite.

Metal ion	k_d at different pH ($\times 10^3$ mL/g)					
	2	3	4	5	6	7
Cu(II)	2.575	12.241	33.461	120	495	620

pH = 6, concentration of metal ions = 10 mg/L, adsorbent dose = 10 mg, and time = 15 min.

where V is the volume of the solution (mL) and m is the weight of adsorbent (g). Initial and final concentrations of the Cu(II) ions in the solutions were measured by AAS. Table 1 shows the k_d value for adsorption of single metal ions. In the case of the removal of Cu(II) ions by PGMA-MAn/ABSAc@Fe_3O_4 nanocomposite, the results indicated that the k_d value is approximately high which proved that metal ions have been retained by the adsorbent.

3.6. Desorption Studies. For potential practical applications, the regeneration and reuse of an adsorbent are important. From the pH study, it has been determined that the adsorption of copper ions on the synthesized nanocomposite tested at pH < 2.0 was negligible at about 15%. This suggested that desorption of copper ions from this magnetic adsorbent was possible around pH lower than 2. For investigation of desorption process, HCl solutions with different pH (1, 1.5, and 2) were used. In Figure 11 it can be seen that the desorption percentages were 91, 85, and 69% for the synthesized nanocomposite in the HCl solutions of pH 1, 1.5, and 2, respectively. The higher desorption efficiency at pH 1 could be referred to the sufficiently high hydrogen ion concentration, which led to the strong competitive adsorption and protonation of active sites. The efficiency of this nanocomposite was determined in adsorption-desorption process for three times (achieved to 81%).

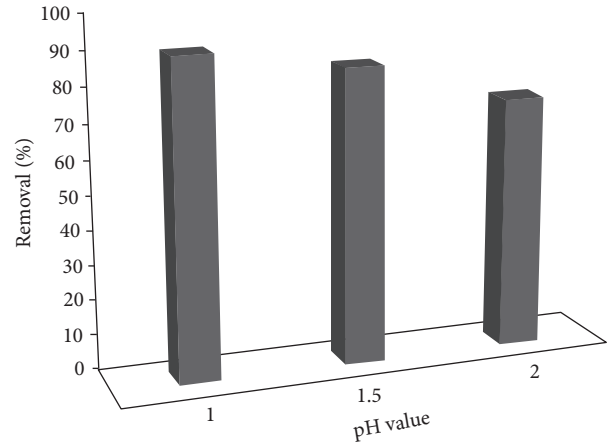

Figure 11: Effect of pH on the regeneration of PGMA-MAn/ABSAc@Fe_3O_4 nanocomposite.

3.7. Comparison with Other Adsorbents. Comparative information on removal of Cu(II) with those of other published results is given in Table 2. The comparative results show that the removal efficiencies of the prepared adsorbent were comparable or higher, in some cases, than the most reported adsorbents in Table 2. Moreover, it was noted that the contact time required for the metal adsorption using this adsorbent was short and the adsorption equilibriums were reached within few minutes for ionic species examined.

Table 2: Comparison of adsorption capacity by various adsorbents for Cu(II) ion adsorptions.

Adsorbents	Cu(II)	Shaking time (min)	Ref.
Nagnetic porous Ferro spinel Mn Fe_2O_4	37.6	180	[18]
EDTA-modified chitosan/SiO_2/Fe_3O_4	44.4	360	[19]
PAA-coated Fe_3O_4	12.4	60	[20]
1,6-Hexadiamine-Fe_3O_4	25.8	5	[21]
Diamine modified mesoporous silica on MWCNTs	66.6	180	[22]
Fe_3O_4@ MCM-41-NH_2	93.0	5	[23]
PGMA-MAn-ABSAc/Fe_3O_4–NH_2	49.51	15	This work

4. Conclusions

In this study, a novel magnetic chelating adsorbent was prepared using reaction of reactive PGMA-MAn copolymer, ABSAc, MNPs-NH_2, and 1,2-ethanedithiol. The synthesized materials were characterized by FT-IR, SEM, EDX, XRD, BET, TGA, and VSM. The adsorption capability of Cu(II) by magnetic chelating adsorbent was investigated. The obtained results can be concluded as follows:

(i) The obtained results from the TGA and VSM of the bare Fe_3O_4 before and after coating clearly indicated that coating procedure was successfully performed.

(ii) The FT-IR, SEM and EDX analyses were shown successful synthesis of magnetic nanocomposite.

(iii) Cu(II) adsorption rate was found to be quite fast and the equilibrium could be achieved within 15 min.

(iv) PGMA-MAn-ABSAc/Fe_3O_4–NH_2 nanocomposite can be used to remove Cu(II) ions via adsorption at pH 6 while regenerated via desorption at pH 1.

(v) Maximum adsorption percentage was obtained at pH between 5 and 6.

(vi) The obtained results showed rapid and effective favored adsorption method for the removal of Cu(II) ions.

Competing Interests

The authors declare that they have no competing interests.

Acknowledgments

The authors are grateful to Azita Hoseinzadeh at the Urmia Water and Wastewater Society and Mehrdad Akhgari at the Department of Analytical Chemistry in Urmia University. The authors are grateful to Iran Polymer and Petrochemical Institute for characterization analyses.

References

[1] M. M. Rao, G. P. C. Rao, K. Seshaiah, N. V. Choudary, and M. C. Wang, "Activated carbon from *Ceiba pentandra* hulls, an agricultural waste, as an adsorbent in the removal of lead and zinc from aqueous solutions," *Waste Management*, vol. 28, no. 5, pp. 849–858, 2008.

[2] M. E. Mahmoud, A. A. Yakout, H. Abdel-Aal, and M. M. Osman, "High performance SiO_2-nanoparticles-immobilized-*Penicillium funiculosum* for bioaccumulation and solid phase extraction of lead," *Bioresource Technology*, vol. 106, pp. 125–132, 2012.

[3] A. Farghali, M. Bahgat, A. E. Allah, and M. Khedr, "Adsorption of Pb(II) ions from aqueous solutions using copper oxide nanostructures," *Beni-Suef University Journal of Basic and Applied Sciences*, vol. 2, no. 2, pp. 61–71, 2013.

[4] M. K. Sahu, S. Mandal, S. S. Dash, P. Badhai, and R. K. Patel, "Removal of Pb(II) from aqueous solution by acid activated red mud," *Journal of Environmental Chemical Engineering*, vol. 1, no. 4, pp. 1315–1324, 2013.

[5] S. Burchi, "Shared natural resources in the European Economic Community legislation," *Natural Resources Journal*, vol. 25, no. 3, pp. 639–649, 1985.

[6] M. Sittig, *Environmental Sources and Emissions Handbook*, Harvard, 18th edition, 1975.

[7] O. Moradi, B. Mirza, M. Norouzi, and A. Fakhri, "Removal of Co(II), Cu(II) and Pb(II) ions by polymer based 2-hydroxyethyl methacrylate: thermodynamics and desorption studies," *Iranian Journal of Environmental Health Science & Engineering*, vol. 9, no. 1, article 31, 2012.

[8] M. A. Barakat, "New trends in removing heavy metals from industrial wastewater," *Arabian Journal of Chemistry*, vol. 4, no. 4, pp. 361–377, 2011.

[9] G.-P. Jin, X.-H. Zhu, C.-Y. Li, Y. Fu, J.-X. Guan, and X.-P. Wu, "Tetraoxalyl ethylenediamine melamine resin functionalized coconut active charcoal for adsorptive removal of Ni(II), Pb(II) and Cd(II) from their aqueous solution," *Journal of Environmental Chemical Engineering*, vol. 1, no. 4, pp. 736–745, 2013.

[10] Q. Su, B. Pan, B. Pan et al., "Fabrication of polymer-supported nanosized hydrous manganese dioxide (HMO) for enhanced lead removal from waters," *Science of the Total Environment*, vol. 407, no. 21, pp. 5471–5477, 2009.

[11] R. Hasanzadeh, P. Najafi Moghadam, and N. Samadi, "Synthesis and application of modified poly (styrene-alt-maleic anhydride) networks as a nano chelating resin for uptake of heavy metal ions," *Polymers for Advanced Technologies*, vol. 24, no. 1, pp. 34–41, 2013.

[12] N. Samadi, R. Hasanzadeh, and M. Rasad, "Adsorption isotherms, kinetic, and desorption studies on removal of toxic metal ions from aqueous solutions by polymeric adsorbent," *Journal of Applied Polymer Science*, vol. 132, no. 11, Article ID 41642, 2015.

[13] F. Zhao, E. Repo, D. Yin, Y. Meng, S. Jafari, and M. Sillanpää, "EDTA-cross-linked β-cyclodextrin: an environmentally friendly bifunctional adsorbent for simultaneous adsorption of

metals and cationic dyes," *Environmental Science & Technology*, vol. 49, no. 17, pp. 10570–10580, 2015.

[14] F. Zhao, E. Repo, Y. Meng, X. Wang, D. Yin, and M. Sillanpää, "An EDTA-β-cyclodextrin material for the adsorption of rare earth elements and its application in preconcentration of rare earth elements in seawater," *Journal of Colloid and Interface Science*, vol. 465, pp. 215–224, 2016.

[15] F. Ge, M.-M. Li, H. Ye, and B.-X. Zhao, "Effective removal of heavy metal ions Cd^{2+}, Zn^{2+}, Pb^{2+}, Cu^{2+} from aqueous solution by polymer-modified magnetic nanoparticles," *Journal of Hazardous Materials*, vol. 211, pp. 366–372, 2012.

[16] Y.-G. Zhao, X.-H. Chen, S.-D. Pan, H. Zhu, H.-Y. Shen, and M.-C. Jin, "Self-assembly of a surface bisphenol A-imprinted core–shell nanoring amino-functionalized superparamagnetic polymer," *Journal of Materials Chemistry A*, vol. 1, no. 38, pp. 11648–11658, 2013.

[17] H. Shen, Z. Wang, A. Zhou et al., "Adsorption of phosphate onto amine functionalized nano-sized magnetic polymer adsorbents: mechanism and magnetic effects," *RSC Advances*, vol. 5, no. 28, pp. 22080–22090, 2015.

[18] Y. Ren, N. Li, J. Feng et al., "Adsorption of Pb(II) and Cu(II) from aqueous solution on magnetic porous ferrospinel $MnFe_2O_4$," *Journal of Colloid and Interface Science*, vol. 367, no. 1, pp. 415–421, 2012.

[19] Y. Ren, H. A. Abbood, F. He, H. Peng, and K. Huang, "Magnetic EDTA-modified chitosan/SiO_2/Fe_3O_4 adsorbent: preparation, characterization, and application in heavy metal adsorption," *Chemical Engineering Journal*, vol. 226, pp. 300–311, 2013.

[20] S.-H. Huang and D.-H. Chen, "Rapid removal of heavy metal cations and anions from aqueous solutions by an amino-functionalized magnetic nano-adsorbent," *Journal of Hazardous Materials*, vol. 163, no. 1, pp. 174–179, 2009.

[21] Y.-M. Hao, C. Man, and Z.-B. Hu, "Effective removal of Cu (II) ions from aqueous solution by amino-functionalized magnetic nanoparticles," *Journal of Hazardous Materials*, vol. 184, no. 1–3, pp. 392–399, 2010.

[22] W. Yang, P. Ding, L. Zhou, J. Yu, X. Chen, and F. Jiao, "Preparation of diamine modified mesoporous silica on multi-walled carbon nanotubes for the adsorption of heavy metals in aqueous solution," *Applied Surface Science*, vol. 282, pp. 38–45, 2013.

[23] A. Mehdinia, S. Shegefti, and F. Shemirani, "Removal of lead(II), copper(II) and zinc(II) ions from aqueous solutions using magnetic amine-functionalized mesoporous silica nanocomposites," *Journal of the Brazilian Chemical Society*, vol. 26, no. 11, pp. 2249–2257, 2015.

[24] H. Shen, S. Pan, Y. Zhang, X. Huang, and H. Gong, "A new insight on the adsorption mechanism of amino-functionalized nano-Fe_3O_4 magnetic polymers in Cu(II), Cr(VI) co-existing water system," *Chemical Engineering Journal*, vol. 183, pp. 180–191, 2012.

[25] H. Shen, J. Chen, H. Dai, L. Wang, M. Hu, and Q. Xia, "New insights into the sorption and detoxification of chromium(VI) by tetraethylenepentamine functionalized nanosized magnetic polymer adsorbents: mechanism and pH effect," *Industrial & Engineering Chemistry Research*, vol. 52, no. 36, pp. 12723–12732, 2013.

[26] K. Zargoosh, H. Habibi, A. Abdolmaleki, and K. Firouz, "Novel magnetic polyamic hydrazide nanocomposite: preparation, characterization, and application for the removal of Cd^{2+} and Pb^{2+} from industrial wastes," *Journal of Applied Polymer Science*, vol. 132, no. 37, Article ID 42538, 2015.

[27] M. M. Lakouraj, F. Mojerlou, and E. N. Zare, "Nanogel and superparamagnetic nanocomposite based on sodium alginate for sorption of heavy metal ions," *Carbohydrate Polymers*, vol. 106, no. 1, pp. 34–41, 2014.

[28] E. N. Zare, M. M. Lakouraj, and A. Ramezani, "Efficient sorption of Pb(II) from an aqueous solution using a poly(aniline-*co*-3-aminobenzoic acid)-based magnetic core-shell nanocomposite," *New Journal of Chemistry*, vol. 40, pp. 2521–2529, 2016.

[29] E. N. Zare, M. M. Lakouraj, and A. Ramezani, "Effective adsorption of heavy metal cations by superparamagnetic poly (aniline–*co*–*m*–phenylenediamine)@ Fe_3O_4 nanocomposite," *Advances in Polymer Technology*, vol. 34, no. 3, 2015.

[30] A. Malekpour and M. Khodadadi, "Albumin-functionalized magnetic nanoparticles as an efficient sorbent for removal of Pb(ii), Cd(ii), Cu(ii) and Cr(vi) ions from aqueous solutions," *RSC Advances*, vol. 6, no. 18, pp. 14705–14711, 2016.

[31] E. K. Oikonomou, G. Bokias, and J. K. Kallitsis, "Comparative study of electrostatic binding vs. complexation of Cu^{2+} ions with water-soluble polymers containing styrene sulphonic acid and/or maleic acid units or their sodium salt forms," *Journal of Polymer Science Part B: Polymer Physics*, vol. 46, no. 12, pp. 1149–1158, 2008.

[32] P. N. Moghadam, R. Hasanzadeh, and J. Khalafy, "Preparation of SMA functionalized sulfanilic acid hydrogels and investigation of their metal ions adsorption behavior," *Iranian Polymer Journal*, vol. 22, no. 2, pp. 133–142, 2013.

[33] R. Hasanzadeh, P. N. Moghadam, N. Bahri-Laleh, and F. Ziaee, "A reactive copolymer based on Glycidylmethacrylate and Maleic Anhydride: 1-synthesis, characterization and monomer reactivity ratios," *Journal of Polymer Research*, vol. 23, no. 8, pp. 150–169, 2016.

[34] M. Ozmen, K. Can, G. Arslan, A. Tor, Y. Cengeloglu, and M. Ersoz, "Adsorption of Cu(II) from aqueous solution by using modified Fe_3O_4 magnetic nanoparticles," *Desalination*, vol. 254, no. 1–3, pp. 162–169, 2010.

[35] W. Lu, Y. Shen, A. Xie, X. Zhang, and W. Chang, "Novel bifuncitonal one-dimensional Fe_3O_4/Se nanocomposites via facile green synthesis," *The Journal of Physical Chemistry C*, vol. 114, no. 11, pp. 4846–4851, 2010.

[36] P. N. Moghadam, R. Hasanzadeh, F. Fathi, and N. Nasr, "Comparative study for adsorption of AL(III) ions from aqueous solutions with series of nano functional copolymers," *Journal of Macromolecular Science, Part A: Pure and Applied Chemistry*, vol. 50, no. 12, pp. 1167–1181, 2013.